repiSalud
Repositorio Institucional en Salud

This is the peer reviewed version of the following article:

AKT and JUN are differentially activated in mesenchymal stem cells after infection with human and canine oncolytic adenoviruses

Miguel Ángel Rodríguez-Milla, Alvaro Morales-Molina, Ana Judith Perisé-Barrios, Teresa Cejalvo, Javier García-Castro.

Cancer Gene Ther. 2020 May 27

which has been published in final form at

https://doi.org/10.1038/s41417-020-0184-9

AKT and JUN are Differentially Activated in Mesenchymal Stem Cells after Infection with Human and Canine Oncolytic Adenoviruses

Miguel Ángel Rodríguez-Milla[1], Alvaro Morales-Molina[1], Ana Judith Perisé-Barrios[1,2], Teresa Cejalvo[1] and Javier García-Castro[1]

[1] Cellular Biotechnology Unit, Instituto de Salud Carlos III, 28220 Madrid, Spain

[2] Biomedical Research Unit, Universidad Alfonso X el Sabio, 28691 Madrid, Spain

Correspondence should be addressed to J.G-C. (jgcastro@isciii.es)

Contact Information:
Javier García-Castro, PhD.
Instituto de Salud Carlos III
Lab. 51-00-031
Ctra. Majadahonda-Pozuelo, Km 2
E-28220 - Majadahonda (Madrid)
Spain

Phone: +34918223288
Fax: +34918223269
E-mail: jgcastro@isciii.es

Abstract

There is increasing evidence about the use of oncolytic adenoviruses (Ads) as promising immunotherapy agents. We have previously demonstrated the clinical efficiency of mesenchymal stem cells (MSCs) infected with oncolytic Ads as an antitumoral immunotherapy (called Celyvir) in human and canine patients, using ICOVIR-5 or ICOCAV17 as human and canine oncolytic Ads, respectively. Considering the better clinical outcomes of canine patients, in this study we searched for differences in cellular responses of human and canine MSCs to Ad infection that may help understand the mechanisms leading to higher antitumor immune response. We found that infection of human and canine MSCs with ICOVIR-5 or ICOCAV17 did not activate the NF-κB pathway or the interferon regulatory factors IRF3 and IRF7. However, we observed differences in the profile of cytokines secretion, as infection of canine MSCs with ICOCAV17 resulted in lower secretion of several cytokines. Moreover, we showed that infection of human MSCs with ICOVIR-5 increased the phosphorylation of a number of proteins, including AKT and cJUN. Finally, we demonstrated that differences in regulation of AKT and cJUN in human and canine MSCs by ICOVIR-5 or ICOCAV17 are intrinsic to each virus. Our findings suggest that ICOCAV17 induces a more limited host response in canine MSCs, which may be related to a better clinical outcome. This result opens the possibility to develop new human oncolytic Ads with these specific properties. In addition, this improvement could be imitated by selecting specific human MSC on the basis of a limited host response after Ad infection.

Keywords: Mesenchymal cells, Canine, Human, Adenovirus, Oncolytic virus, AKT, JUN

Introduction

The use of oncolytic viruses is an immunotherapy treatment for cancer that uses viruses designed to infect and/or replicate specifically in tumor cells. Recently, Imlygic, an oncolytic virus based in herpex virus, received the approval from the FDA and EMA to be used intratumorally in melanoma patients (1). However, very limited efficacy has been observed in clinical studies using intravenous delivery of oncolytic viruses. With the aim to target metastatic or widespread cancer we have developed a “Trojan horse” strategy using cellular-vehicles to deliver oncolytic virus intravenously. In this regard, we have previously demonstrated the efficiency of mesenchymal stem cells (MSCs) infected with oncolytic adenoviruses (Ads) as an antitumoral immunotherapy that we called Celyvir. Thus, we reported an initial clinical experience of this treatment related with a program of compassionate use and a clinical trial in pediatric patients (NCT01844661) showing an excellent toxicity profile and several clinical responses, including two complete remissions (2-4). More recently, we improved our immunotherapy in mice models (5, 6) and finally we tested these improvements in dogs with spontaneous tumors in a veterinary clinical trial (7). Naturally occurring cancers in pet dogs and humans share many features, including histological appearance, tumor genetics, molecular targets, biological behavior and response to conventional therapies (8). Thus, in our veterinary trial including 27 canine patients treated with dCelyvir, we used dog MSCs (dMSCs) infected with ICOCAV17 –a canine adenovirus homologous to human ICOVIR-5– and we observed a clinical benefit in 74% of patients, including 14.8% showing complete remissions (7).

Although we have demonstrated the clinical efficacy of Celyvir, it is necessary to further explore its mechanism of action to improve its benefits. The basic elements of Ad intracellular trafficking have been described although differences have been noted related with variations based on Ad serotype, target cell type, and cell physiology (9). In non-immune cells, signalling events activated by Ad infection are relatively well studied (e.g., PI3K, p38, ERK and NF-κB) and although these cells may contribute to certain Ad innate reactions, the majority of these responses are originated from cells of the innate immune system such as macrophages and dendritic cells (10). This associated immune response is also influenced by the virus type, cell type and host species (11) and includes: activation of a systemic pro-inflammatory state, attracting cytotoxic immune cell populations to the sites of infection to eliminate virus-containing cells, and alarming neighboring uninfected cells of viral infection (12).

Several groups have observed specific effects after transduction of human cells with human and canine adenoviral vectors (13, 14). Here we compared the effects of human MSCs (hMSCs) infected with ICOVIR-5 in signaling pathways to those of dMSCs infected with ICOCAV17. Considering the better clinical outcomes of dCelyvir, the observed differences have the potential to help understand the mechanisms leading to increase the clinical efficacy of Celyvir.

Materials and methods

Cell lines and cell culture. hMSCs were purchased from Lonza (Basel, Switzerland) and cultured either in Mesenchymal Stem Cell Growth Medium (MSCGM) and the necessary supplements or in Dulbecco's Modified Eagle's Media (DMEM) supplemented with heat-inactivated 10% fetal bovine serum

(FBS), 2 mM glutamine, streptomycin (100 mg/mL) and penicillin (100 U/mL) (complete DMEM). dMSCs and the DK28Cre cell line were obtained as indicated in (7) and cultured in complete DMEM. HEK293 cells were cultured in complete DMEM. All cell lines were maintained under standard conditions (5% CO_2, 37°C) in their appropriate medium and routinely tested for mycoplasma contamination using the MycoAlert Micoplasm Detection Kit (Lonza). All culture reactives were obtained from Lonza with the exception of FBS, which was purchased from Sigma (St. Louis, MO, USA).

Adenovirus. ICOVIR-5 and ICOCAV17 have been extensively described elsewhere (15, 16), respectively. CAV2-GFP is a canine non replicative adenoviral vector expressing GFP and was purchased from the Viral Vector Production Unit at Universitat Autonoma de Barcelona, Spain. All Ads were generated by the transfection of linearized plasmid into HEK293 (ICOVIR-5) or DK28Cre cells (ICOCAV17 and CAV2-GFP) and purified by CsCl gradient centrifugation.

Infection of MSCs, HEK293 and DK28Cre. Unless otherwise stated, MSCs were infected at different multiplicity of infection (MOI) in serum-free DMEM for 2h at 37°C, washed with PBS, seeded and incubated in complete DMEM at 37°C for the required time points. For analysis of viral production, human and canine MSCs were infected with ICOVIR-5 and ICOCAV17 for three days, then cells and medium were harvested and the virus particles released by three repeated freeze-thaw cycles. Cell debris were removed by centrifugation at 1200 rpm for 5 min and filtered through a 0.45 µm filter. Then, HEK293 cells (for amplification of ICOVIR-5) or DK28Cre cells (for amplification of ICOCAV17) were seeded in 24-well plates and infected with the appropriate cell-free extract. Cells were

examined every day for cytopathic effects using a Leica DM IL LED microscope (Leica Microsystems, Wetzlar, Germany). CAV2-GFP infected cells were analyzed using the Leica TCS SP5 multispectral confocal microscope (Leica Microsystems) and representative images were obtained by maximum projection of 4 stacks.

Quantitation of viral DNA by qPCR. ICOVIR-5 and ICOCAV17 genome copy number was quantified by Quantitative Real Time-PCR as previously described (17). Briefly, total DNA from cell culture supernatants was isolated by the QIAamp DNA Mini Kit (QIAGEN, Valencia, CA) according to the manufacturer´s instructions. Five microliters of DNA were used for Real Time-PCR using the primers ICO5F2: GAT TTG GCG CGT AAA AGT G and ICO5R2: CGG CCA TTT CTT CGG TAA TA for ICOVIR-5 and CAV2-F: CGT GAA GCG CCG TAG ATG C and CAV2-R: GAA CCA GGG CGG GAG ACA AGT ATT for ICOCAV17. Real Time PCR consisting of 10 min at 95ºC and 40 cycles (95ºC, 10 s; 60ºC 10 s; 72ºC, 18 s) was performed on the LightCycler 1.5 Real Time PCR Thermal Cycler (Roche, Basel, Switzerland), using LightCycler FastStart Essential DNA Green Master (Roche) and analyzed with LightCycler Software 3.5 (Roche). A qPCR standard curve was generated using 10-fold serial dilutions of ICOVIR-5 and ICOCAV17 plasmid DNA and the copy number present in the sample was obtained by extrapolation of the Ct value on the standard curve. Two independent experiments with different MSC donors were performed.

Luciferase assays. The activation of NF-κB pathway was determined using a luciferase reporter system (18). Replication incompetent lentiviral vectors were created using the pHAGE NF-κB-TA-LUC-UBC-GFP-W plasmid, a gift from Darrell Kotton (Addgene plasmid #49343). The plasmid encodes the NF-κB

158 consensus binding sequence upstream of the minimal TA promoter of the herpes
159 simplex virus followed by the firefly luciferase gene as well as the eGFP gene
160 upstream of the ubiquitin-C promoter. Transduction of MSCs was performed
161 overnight and GFP expression was assessed by flow cytometry. For luciferase-
162 reporter assays, control and adenovirus infected cells were lysed and luciferase
163 activity was assayed with the Luciferase Assay System (Promega, Madison, WI,
164 USA) according to the manufacturer's instructions. Three independent
165 experiments with different MSC donors were performed.

166 **Western blot analysis.** Total proteins were extracted with SDS sample buffer
167 (62.5 mM Tris pH 6.8, 2% SDS, 10% glycerol, 1 mM phenylmethylsulfonyl fluoride
168 [PMSF], 5 mM NaF, 20 mM β-glycerophosphate, 0.1 mM Na_3VO_4, and 1:100
169 protease inhibitor cocktail from Sigma). Then, samples were boiled and
170 sonicated. Nuclear extracts were prepared using the Nuclear Extraction Kit
171 (Abcam, *Cambridge*, UK) according to the manufacturer's instructions. Primary
172 antibodies were mouse monoclonal anti-c-Jun (phospho S63) 1:1000 dilution
173 (Santa Cruz Biotechnology Inc., Santa Cruz, CA, USA), rabbit monoclonal anti-
174 AKT1 (phospho S473) antibody, 1:1000 dilution (Epitomics, Burlingame, CA,
175 USA), rabbit polyclonal anti-RelB 1:200 dilution (Santa Cruz Biotechnology Inc.),
176 rabbit polyclonal anti-IκB-α 1:200 dilution (Santa Cruz Biotechnology Inc.), and
177 mouse monoclonal anti-β-actin, 1:100000 dilution (Sigma). Secondary antibodies
178 were polyclonal goat anti-rabbit and anti-mouse immunoglobulins/HRP, 1:3000
179 dilution (DAKO, Carpinteria, CA, USA). Two independent experiments with
180 different MSC donors were performed.

181 **Cytokine and phospho-kinase array analysis.** For the analysis of the cytokine
182 pattern in both hMSCs and dMSCs after adenovirus infection, the Human XL

Cytokine Array kit (R&D Systems, Minneapolis, MN, USA) was used according to manufacturer's recommendation. The array consisted of 102 different human cytokine antibodies spotted in duplicate onto a nitrocellulose membrane. hMSCs and dMSCs from two different donors were first seeded on 6-well dishes at a density of 10^5 and 2×10^5 cells/well, respectively. Then, they were infected for 1.5 h, washed with PBS and incubated in serum-free DMEM for 3 h or 24 h. Finally, supernatants from either control or adenovirus infected samples were collected, centrifuged to eliminate dead cells and debris and the protein pattern was analyzed using proteome profiler array kits. The phosphorylation profile in MSCs after adenovirus infection was analyzed using the Proteome Profiler Human Phospho-Kinase Array (R&D Systems) according to the manufacturer's instructions. This array detects phosphorylation of 43 human kinases and total amounts of 2 related proteins. Cell lysates (400 µg) from either control or adenovirus infected samples were incubated with each set of nitrocellulose membranes of the Human Phospho-Kinase Array with the spotted capture antibodies. Array images were scanned and digitized, and integrated pixel density of the spots was quantified using the Fiji software. The average density of duplicated spots representing each protein was used to determine changes in expression of cytokines or phosphorylated proteins after adenoviral infection. Differentially expressed proteins were further studied with STRING software (19) to analyze the biological process and reactome pathways in which they are involved.

Statistical analysis. Data was analyzed and graphed using GraphPad Prism (GraphPad Software, San Diego. CA, USA). Statistical significance was

determined using unpaired t-test: $p < 0.05$ (*), $p < 0.01$ (**), $p < 0.001$ (***) and $p < 0.0001$ (****).

Results

Infection of MSCs with ICOVIR-5 and ICOCAV17 does not activate either NF-κB pathway or interferon regulatory factors IRF3 and IRF7

In order to compare the effects of ICOVIR-5 and ICOCAV17 infection of hMSCs and dMSCs, respectively, we first studied the sensitivity of both cells to each Ad. For the clinical trial of hCelyvir, ICOVIR-5 was used at a MOI of 200 PFU/cell because that was the average MOI obtained in previous studies for the infection of hMSCs from different donors (4). For our veterinary trial of dCelyvir (7), we used ICOCAV17 at a MOI of 1 PFU/cell based in previous results using this oncolytic Ads, where the IC50 values infecting canine tumoral cell lines ranked 0,5-15 PFU/cell (16). Thus, we compared hMSCs and dMSCs infected at these MOIs and observed that they were infected to an equivalent degree (Supplementary Fig. S1). First, Ad infection caused similar cytopathic effects (CPE), which started at 2 days post-infection. In addition, Ad titers obtained from supernatant cultures were comparable (Fig. 1a). However, when hMSCs were infected at 1 PFU/cell no detectable CPE was observed whereas infection of dMSCs at 200 PFU/cell caused excessive early CPE (Supplementary Fig. S1). Therefore, as our goal was to compare Ad-induced effects in MSCs in hCelyvir and dCelyvir under clinical conditions (healthy MSCs able to undergo tumor-homing during 24-48 h post-infection), we performed all the experiments under the conditions previously published.

Ad infection leads to the activation of intracellular signaling cascades as a virus-induced innate response of the cells (10). We first searched for Ad-induced differences in immune-related pathways in hMSCs and dMSCs. Because NF-κB is classically activated by Ads and activates numerous early response genes, including genes encoding for inflammatory cytokines and chemokines (20), we studied its activation using a lentiviral vector expressing a luciferase reporter gene under a NF-κB promoter. No significant differences in luciferase levels were observed at the times studied in either type of cell (Fig.1a, b). Similarly, immunoblotting experiments revealed that proteins involved in the induction of the canonical (IκB-α) and non-canonical (RelB) NF-κB pathways as well as interferon regulatory factors IRF3 and IRF7, which activate the transcription of IFN-α or IFN-β, respectively, were constitutively expressed at similar levels in infected cells compared to the control (Fig. 1c-f). Nevertheless, we observed a slight decrease in IκB-α in hMSCs after 24 hours of infection consistent with the small increase in luciferase levels shown in Fig.1a.

Analysis of cytokines in MSCs displays different secretion profiles

Next, we investigated the profiles of cytokine secretion in MSCs in response to Ad infection using a human cytokine antibody array, as other human arrays have been successfully used in the analysis of canine samples (21). Overall, a more complex profile was detected at 3 hours post-infection compared to 24 hours. Thus, at 3 hours, signal above background level was detected in hMSCs for all 105 cytokines implemented in the array compared with 71 in dMSCs (Fig. 2a). However, after 24 hours, signal was detected only for 41 cytokines in hMSCs compared with 19 in dMSCs (Fig. 2b). When we compared ICOVIR-5-infected hMSCs to ICOCAV17-infected dMSCs, no major differences were found on the

levels of secreted cytokines. Thus, the array included well characterized pro-inflammatory cytokines (IL-1, IL-6, IL-8, IL-12, IFN-γ, IL-18, and TNF) whose analysis showed no significant differences between infected and control samples (Fig. 2a-b). This is consistent with the lack of activation of NF-κB pathway observed above (Fig. 1a-d). Nevertheless, there were significant differences in fold-change of four cytokines (ST2, TARC, THBS1 and µPAR) after Ad-infection, showing a higher down-regulated expression in ICOCAV17-infected dMSCs compared to ICOVIR-5-infected hMSCs (Fig. 2c, d).

AKT and JUN are differentially regulated in hMSCs and dMSCs after infection with ICOVIR-5 and ICOCAV17

To determine whether other signaling pathways were altered by Ad infection in MSCs, since Ad-induced phosphorylation of several proteins is well described (10), we utilized a human phospho-kinase array to detect changes in phosphorylation profiles of kinases and their substrates. hMSCs and dMSCs were infected with ICOVIR-5 and ICOCAV17 and phosphorylation profiles analyzed at 3 and 24 hours postinfection (Fig. 3a, b). Analysis of phosphorylation profiles in ICOVIR-5-infected hMSCs compared to ICOCAV17-infected dMSCs resulted in some significant changes at 3 and 24 hours postinfection (Fig. 3c, d) although the differences observed were very small in most cases (especially at 3 hours). However, after 24 hours, ICOVIR-5 and ICOCAV17 infection of hMSCs and dMSCs resulted in strong contrasting effects on the phosphorylation levels of AKT (fold change: 33.3 in hMSCs compared to -0.3 in dMSCs) and c-JUN (fold change: 1.4 in hMSC compared to -1 in dMSCs). Similar significant results were observed for GSK-3 α/β and CREB. Considering the well-known roles of the AKT and c-JUN pathways during Ad infection (10), we further validated the expression

of both proteins in different donors using western blot analysis (Supplementary Figure S2). Consistent with the results from the array, phosphorylation of both AKT and c-JUN in hMSCs infected with ICOVIR-5 increased at 24 hours postinfection. In contrast, none pathway was activated in dMSCs infected with ICOCAV17. In both cases the observed changes were dose dependent.

STRING analysis depicted networks of interactions of the significantly higher secreted cytokines and phosphorylated proteins in infected hMSC compared to infected dMSC at 3 hours (Fig. 3e) and 24 hours (Fig. 3f). Gene Ontology enrichment analyses identified biological processes that are associated with positive regulation of cellular process, negative regulation of cell death, regulation of apoptosis and regulation of autophagy.

Regulation of AKT and JUN in hMSCs and dMSCs by ICOVIR-5 or ICOCAV17 infection is intrinsic to each specific adenovirus

Considering the contrasting differences observed between human and canine Ads in AKT and c-JUN phosphorylation, we further tested whether these responses were host- or Ad-specific. We then performed host-cross infections of human and canine adenoviruses (Fig. 4a). We found out that ICOVIR-5 was able to replicate in some degree in dMSCs, as a strong CPE was observed in HEK293 cells infected with virus released from ICOVIR-5-infected dMSCs (Fig. 4a-II). In addition, Ad titers were similar to those obtained for ICOVIR-5-infected hMSCs (Fig. 4b). By contrast, ICOCAV17 infection of hMSCs was very inefficient as the CPE caused to DK28Cre cells infected with virus released from ICOCAV17-infected hMSCs was very weak (Fig. 4a-IV) and Ad titers were very low (Fig. 4b). Indeed, when hMSCs were infected with CAV2-GFP, a non-replicative canine Ad vector, no fluorescence was observed whereas infection

of dMSCs resulted in strong GFP signal (Fig. 4c). Finally, infection of dMSCs with human ICOVIR-5 resulted in a strong phosphorylation of AKT and c-JUN similar to ICOVIR-5-infected hMSCs but no activation of AKT and c-JUN was observed when hMSCs were infected with ICOCAV17 (Fig. 4d).

Discussion

The aim of this study was to identify specific responses induced by ICOVIR-5 and ICOCAV17, human and canine oncolytic Ads respectively, upon infection of MSCs that may be related to the better clinical outcome of dCelyvir. Other studies using human cells infected by human and canine Ads have identified specific responses of each virus (13, 14). By contrast, we searched for differences between ICOVIR-5-infected hMSCs and ICOCAV17-infected dMSC. Our data suggest that NF-κB pathway, interferons and pro-inflammatory cytokine secretion are not the primary sensors of Ad infection in hMSCs and dMSCs. Similarly, it has been shown that transduction of rat MSCs with human adenoviral vectors has no major influence on the expression profile of immunologically relevant parameters (22). Although we observed distinct cytokine secretion profiles, part of the differences observed in our non-infected samples may be due to lack of homology between human and canine cytokines. Nevertheless, we demonstrated that hMSCs and dMSCs displayed Ad-induced changes in the secretion of ST2, TARC, THBS1 and μPAR. These differences found were mostly due to decreased secretion in dCelyvir, not by higher secretion in hCelyvir (with the exception of TARC). Thus, the decrease of these cytokines, together with the overall reduction of cytokine secretion after 24 hours in dMSCs indicates that dCelyvir presents a lower profile of cytokine expression.

Interestingly, when we compared the activation of other important signaling molecules, a number of differentially phosphorylated targets were identified. It is known that many viruses modulate the signaling pathways of the host cell to escape activation of key innate immune mechanisms and establish a productive infection (23). Thus, some viruses activate PI3K–AKT signaling for latent infection and others for short-term cellular survival during the initial stages of acute infection, when virus replication and protein synthesis are taking place (24). Accordingly, our findings that ICOVIR-5 induces a strong phosphorylation of AKT and c-JUN in hMSCs after 24 hours of infection whereas ICOCAV17 does not activate these pathways in dMSCs, indicate that ICOCAV17 induces a more limited host response than ICOVIR-5. The fact that ICOVIR-5, a human Ad, can also activate AKT and c-JUN in canine MSCs demonstrates that these cells can activate these pathways in response to other Ads. These data indicate that the impaired cellular signaling after infection is intrinsic to ICOCAV17. Together with the observed decreased cytokine secretion, the results suggest that ICOCAV17 somehow avoids host cell signaling in dMSCs.

Activation of PI3K/AKT and AP-1 signaling pathways by Ads is well established, and the roles of these pathways in cell survival and apoptosis are known. Remarkably, Ad activation of the PI3K/AKT pathway maintains host cell viability during viral replication and therefore benefits the virus rather than the host (25). Moreover, activation of JUN kinases and AKT has been proposed to be required for Ad-mediated autophagy necessary for their lytic cycle, using □24RGD, an Ad very similar to ICOVIR-5 (26). Binding of the Ad penton base RGD-motif to α_v integrins induces phosphorylation of several signaling proteins, including FAK and PI3K (27), but canine Ads do not contain a RGD motif in their

356 penton base, using the Coxsackie and Ad receptor (CAR) or other primary
357 receptors to bind the cells (28). This absence of RGD(penton base)-integrin
358 interactions would be the cause of this different intracellular activation after
359 ICOVIR-5 and ICOCAV17 infection. However, both Ads include artificial RGD
360 motifs in the H1 loops of their fibers (15, 16). That positioning of the RGD motif
361 within the knob of Ad fiber protein should make this ligand available for efficient
362 interaction with integrins on the cell membrane (29). Nevertheless, so far is not
363 known whether this RGD(Knob)-integrin interaction would generate the same or
364 different intracellular signaling events comparing with RGD(penton base) motifs.

365 Moreover, other authors have also reported altered responses between
366 human and canine Ads after infection of human cells. Thus, transduction of
367 dendritic cells has shown that the canine adenoviral CAV-2 vectors, in contrast
368 to human adenoviral serotype-5 vectors, provoked minimal upregulation of major
369 histocompatibility complex class I/II and costimulatory molecules (CD40, CD80
370 and CD86), and induced negligible morphological changes indicative of dendritic
371 cell maturation (13). Similarly, transduction of neurons with human and canine
372 adenoviral vectors resulted in distinct transcriptome profiles (14). By the other
373 hand, the CAV-2 capsid is approximately 10-fold-less negatively charged than
374 human Ad5 (28). It is possible that the more neutral net charge of the CAV-2
375 capsid induce a different attachment to MSC, with a different signaling induction
376 after infection. In addition, a more flexible CAV-2-CAR interaction compared to
377 human Ad5-CAR has been suggested (30), which would also have a role in
378 cellular attachment, internalization and intracellular signaling.

379 We propose the hypothesis that the absence of activation of AKT and
380 cJUN pathways by ICOCAV17 may result in a more ‘silent’ infection that improves

the efficacy of dCelyvir. Thus, in ICOVIR-5-infected hMSCs, cellular processes induced by AKT/cJUN phosphorylation may prevent the activation of the same mechanisms induced in dCelyvir. It is tempting to speculate that part of these results may be due to functional differences in viral proteins. Besides, clinical responses in human patients were achieved when hMSCs presented a lower pro-inflammatory profile after Ad infection, indicating some degree of natural Ad-sensitivity between patients (31). Our results open the possibility to develop new oncolytic Ads with these specific properties. In addition, this mechanism of action could be imitated in clinical hCelyvir by selecting specific human allogeneic MSCs on the basis of their limited host response after Ad infection.

Acknowledgements

The authors would like to thank Isabel Cubillo Moreno for her technical support in the study.

Conflict of interest

The authors declare that they have no conflict of interest.

Funding

This study was funded by Instituto de Salud Carlos III (PI14CIII/00005 and PI17CIII/00013 grants), Consejería de Educación, Juventud y Deporte of Comunidad de Madrid (P2017/BMD-3692 grant), Fundación Oncohematología Infantil, AFANION and Asociación Pablo Ugarte, whose support we gratefully acknowledge.

References

1. Garnock-Jones K. Talimogene Laherparepvec: A Review in Unresectable Metastatic Melanoma. BioDrugs. 2016;30:461-8.
2. García-Castro J, Alemany R, Cascalló M, Martínez-Quintanilla J, Arriero MM, Lassaletta A, et al. Treatment of metastatic neuroblastoma with systemic oncolytic virotherapy delivered by autologous mesenchymal stem cells: an exploratory study. Cancer Gene Ther. 2010;17:476-83.
3. Melen GJ, Franco-Luzon L, Ruano D, Gonzalez-Murillo A, Alfranca A, Casco F, et al. Influence of carrier cells on the clinical outcome of children with neuroblastoma treated with high dose of oncolytic adenovirus delivered in mesenchymal stem cells. Cancer Lett. 2016;371(2):161-70.
4. Ruano D, Lopez-Martin JA, Moreno L, Lassaletta A, Bautista F, Andion M, et al. First-in-Human, First-in-Child Trial of Autologous MSCs Carrying the Oncolytic Virus Icovir-5 in Patients with Advanced Tumors. Mol Ther. 2020;28(4):1033-42.
5. Rincón E, Cejalvo T, Kanojia D, Alfranca A, Rodríguez-Milla MA, Gil Hoyos RA, et al. Mesenchymal stem cell carriers enhance antitumor efficacy of oncolytic adenoviruses in an immunocompetent mouse model. Oncotarget. 2017;8:45415-31
6. Morales-Molina A, Gambera S, Cejalvo T, Moreno R, Rodriguez-Milla MA, Perise-Barrios AJ, et al. Antitumor virotherapy using syngeneic or allogeneic mesenchymal stem cell carriers induces systemic immune response and intratumoral leukocyte infiltration in mice. Cancer Immunol Immunother. 2018;67(10):1589-602.
7. Cejalvo T, Perisé-Barrios AJ, Portillo Id, Laborda E, Rodriguez-Milla M, Cubillo I, et al. Remission of Spontaneous Canine Tumors after Systemic Cellular Viroimmunotherapy. Cancer Res. 2018;78:4891–901.
8. Paoloni M, Khanna C. Translation of new cancer treatments from pet dogs to humans. Nat Rev Cancer. 2008;8:147-56.

9. Leopold PC, RG. Intracellular trafficking of adenovirus: Many means to many ends. Adv Drug Deliv Rev. 2007;59:810–21.
10. Fejer G, Freudenberg M, Greber U, Gyory I. Adenovirus-triggered innate signalling pathways. Eur Jl of Microbiol and Immunol. 2011;1:279-88.
11. Flatt J, Butcher S. Adenovirus flow in host cell networks. *Open Biol*. 2019;9:190012.
12. Atasheva S, Shayakhmetov D. Adenovirus sensing by the immune system. Curr Opin Virol. 2016;21:109-13.
13. Perreau M, Mennechet F, Serratrice N, Glasgow J, Curiel D, Wodrich H, et al. Contrasting Effects of Human, Canine, and Hybrid Adenovirus Vectors on the Phenotypical and Functional Maturation of Human Dendritic Cells: Implications for Clinical Efficacy. J Virol. 2007;81:3272–84.
14. Piersanti S, Astrologo L, Licursi V, Costa R, Roncaglia E, Gennetier A, et al. Differentiated Neuroprogenitor Cells Incubated with Human or Canine Adenovirus, or Lentiviral Vectors Have Distinct Transcriptome Profiles. PLoS ONE. 2013;8:e69808.
15. Cascallo M, Alonso M, Rojas J, Perez-Gimenez A, Fueyo J, Alemany R. Systemic toxicity-efficacy profile of ICOVIR-5, a potent and selective oncolytic adenovirus based on the pRB pathway. Mol Ther. 2007;15:1607-15.
16. Laborda E, Puig-Saus C, Rodriguez-Garcia A, Moreno R, Cascallo M, Pastor J, et al. A pRb-responsive, RGD-modified, and hyaluronidase-armed canine oncolytic adenovirus for application in veterinary oncology. Mol Ther. 2014;22(5):986-98.
17. Segura MM, Monfar M, Puig M, Mennechet F, Ibanes S, Chillon M. A real-time PCR assay for quantification of canine adenoviral vectors. J Virol Methods. 2010;163(1):129-36.
18. Wilson A, Kwok L, Porter E, Payne J, McElroy G, Ohle S, et al. Lentiviral delivery of RNAi for in vivo lineage-specific modulation of gene expression in mouse lung macrophages. Mol Ther. 2013;21:825-33.

19. Szklarczyk D, Gable AL, Lyon D, Junge A, Wyder S, Huerta-Cepas J, et al. STRING v11: protein-protein association networks with increased coverage, supporting functional discovery in genome-wide experimental datasets. Nucleic Acids Res. 2019;47(D1):D607-d13.
20. Doronin K, Flatt JW, Di Paolo NC, Khare R, Kalyuzhniy O, Acchione M, et al. Coagulation Factor X Activates Innate Immunity to Human Species C Adenovirus. Science. 2012;9:795-8.
21. McCleese J, Bear M, Kulp S, Mazcko C, Khanna C, London C. Met interacts with EGFR and Ron in canine osteosarcoma. Vet Comp Oncol. 2013;11:124–39.
22. Treacy O, Ryan A, Heinzl T, O'Flynn L, Cregg M, Wilk M, et al. Adenoviral Transduction of Mesenchymal Stem Cells: In Vitro Responses and In Vivo Immune Responses after Cell Transplantation. PLoS ONE. 2012;7:e42662.
23. Bowick G, Fennewald S, Scott E, Zhang L, Elsom B, Aronson J, et al. Identification of Differentially Activated Cell-Signaling Networks Associated with Pichinde Virus Pathogenesis by Using Systems Kinomics. *J Virol*. 2007;81:*1923–33*.
24. Cooray S. The pivotal role of phosphatidylinositol 3-kinase–Akt signal transduction in virus survival. J Gen Virol 85:1065–1076.
25. Rajala MS, Rajala RV, Astley RA, Butt AL, Chodosh J. Corneal Cell Survival in Adenovirus Type 19 Infection Requires Phosphoinositide 3-Kinase/Akt Activation. J Virol. 2005;79:12332–41.
26. Klein S, Piya S, Lu Z, Xia Y, Alonso M, White E, et al. C-Jun N-terminal kinases are required for oncolytic adenovirus-mediated autophagy. Oncogene. 2015;34:5295–301.
27. Li E, Stupack D, Klemke R, Cheresh DA, Nemerow GR. Adenovirus Endocytosis via α v Integrins Requires Phosphoinositide-3-OH Kinase. J Virol. 1998;72:2055-61.
28. Soudais C, Boutin S, Hong Sea. Canine adenovirus type 2 attachment and internalization: coxsackievirus-adenovirus receptor, alternative receptors, and an RGD-independent pathway. J Virol 2000;74:10639-49.

487 29. Dmitriev I, Krasnykh V, Miller CR, Wang M, Kashentseva E, Mikheeva G, et al. An
488 adenovirus vector with genetically modified fibers demonstrates expanded tropism
489 via utilization of a coxsackievirus and adenovirus receptor-independent cell entry
490 mechanism. J Virol. 1998;72:9706-13.
491 30. Seiradake E, Lortat-Jacob H, Billet O, Kremer EJ, Cusack S. Structural and
492 mutational analysis of human Ad37 and canine adenovirus 2 fiber heads in
493 complex with the D1 domain of coxsackie and adenovirus receptor. J Biol Chem.
494 2006;281:33704-16.
495 31. Melen G, Franco-Luzón L, Ruano D, González-Murillo A, Alfranca A, Casco F, et al.
496 Influence of carrier cells on the clinical outcome of children with neuroblastoma
497 treated with high dose of oncolytic adenovirus delivered in mesenchymal stem cells.
498 Cancer Letters. 2016;371:161-70.
499

500 **Figure Legends**

501 **Fig. 1 NF-KB signaling pathway activity and IRFs phosphorylation after**
502 **adenoviral infection of human and canine MSCs.** All the experiments were
503 performed using hMSCs infected with ICOVIR-5 (MOI 200 PFU/cell) and dMSCs
504 infected with ICOCAV17 (MOI 1 PFU/cell). **a** Culture supernatants of infected
505 MSC were collected at various times post-infection and Ad titers measured as
506 described in Methods. Graphs show mean + SD (*n* = 3). Ad titers of hMSCs and
507 dMSCs analyzed at the indicated times post-infection. Graphs show mean+SD
508 (*n* = 3) (log_{10} scale). **b** Luciferase activity of hMSCs and dMSCs transduced with
509 the NF-KB-reporter lentiviral vector after Ad infection at the indicated times.
510 Graphs show mean + SD fold increase (*n* = 3). **c**, **d** Western blots of total or
511 nuclear extracts (ne) from hMSCs and dMSCs were probed with the indicated

antibodies. Two independent experiments with different MSC donors were performed.

Fig. 2 Array analysis of secreted cytokines in human and canine MSCs after Ad infection. Serum-free medium from hMSCs infected with ICOVIR-5 (MOI 200 PFU/cell) and dMSCs infected with ICOCAV17 (MOI 1 PFU/cell) for the indicated times was collected and a secretory profile obtained using the Human XL Cytokine Array kit. The heat maps show the detected cytokines above background level in at least one cell type. All 102 cytokines present in the array were identified after 3 h of infection (**a**) whereas only 51 after 24 h (**b**). **c**, **d** Statistical analysis showing differentially expressed cytokines (infected vs. control ratios) in hMSCs (purple) and dMSCs (yellow) in response to Ad infection (T-test: $p < 0.05$) (**c**, 3 h; **d**, 24 h). Two independent experiments with different MSC donors were performed.

Fig. 3 Signaling pathways regulated by Ad infection in human and canine MSCs. a, **b** Heat maps showing phospho-kinase profiles in cell lysates of hMSCs and dMSCs infected with ICOVIR-5 (MOI 200 PFU/cell) or ICOCAV17 (MOI 1 PFU/cell) for the indicated times obtained with the Human Phospho-Kinase Antibody Array. **c**, **d** Statistical analysis showing differentially expressed phospho-kinases in hMSCs and dMSCs in response to Ad infection at 3 (**c**) or 24 h (**d**). (T-test: $p < 0.05$). **e**, **f** Network presenting cytokines with increased infected/control ratios in hMSCs compared to dMSCs at 3 (**e**) and 24 h (**f**). Line thickness indicates the strength of data support between edges. Colors represent the biological process in which the cytokine is involved according to the legend.

Fig. 4 Differences in replication and signaling between ICOVIR-5 and ICOCAV17 depending on cell host. a Scheme showing the experimental design

of host-crossed infections. Bright field micrographs (100X total magnification) showing the cytopathic effect observed in HEK293 or DK28CRE cells with cell-free extracts from hMSCs infected with ICOVIR-5 (MOI 200 PFU/cell) (I), dMSCs infected with ICOVIR-5 (MOI 200 PFU/cell) (II), dMSCs infected with ICOCAV17 (MOI 1 PFU/cell) (III) or hMSCs infected with ICOCAV17 (MOI 1 PFU/cell) (IV). In all cases, cell-free extracts were obtained at 72 h post-infection. Uninfected cells were used as controls. **b** Culture supernatants of hMSCs and dMSCs infected with ICOVIR-5 (MOI 200 PFU/cell) or ICOCAV17 (MOI 1 PFU/cell) were collected at various times post-infection and Ad titers measured as described in Methods. Graphs show mean + SD (*n* = 3) (log_{10} scale). **c** Western blots of dMSCs and hMSCs infected for 24 h with ICOVIR-5 (MOI 200 PFU/cell) or ICOCAV17 (MOI 1 PFU/cell) were probed with the indicated antibodies. **d** Confocal analysis of dMSCs and hMSCs infected with CAV2-GFP (MOI 10 PFU/cell). Positive signal was detected in dMSCs whereas fluorescence was missing in hMSCs.

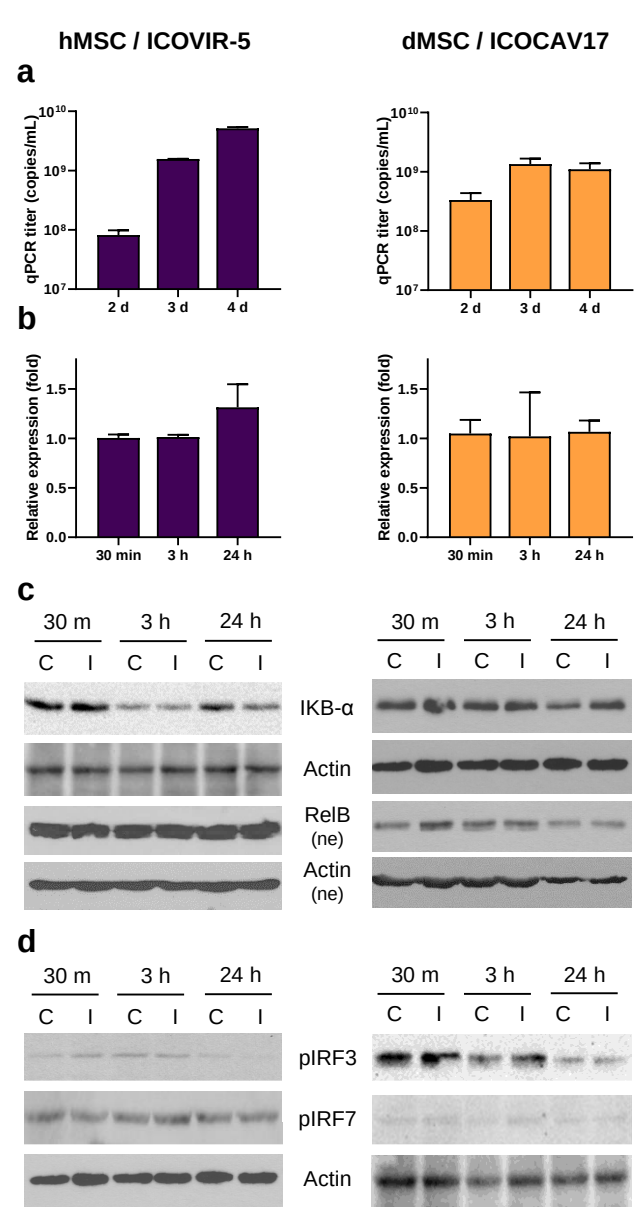
hMSC / ICOVIR-5
dMSC / ICOCAV17
a
qPCR titer (copies/mL)
10^{10}
10^{9}
10^{8}
10^{7}
2 d
3 d
4 d
b
Relative expression (fold)
1.5
1.0
0.5
0.0
30 min
3 h
24 h
c
30 m
3 h
24 h
C
I
IKB-α
Actin
RelB
(ne)
Actin
(ne)
d
pIRF3
pIRF7
Actin

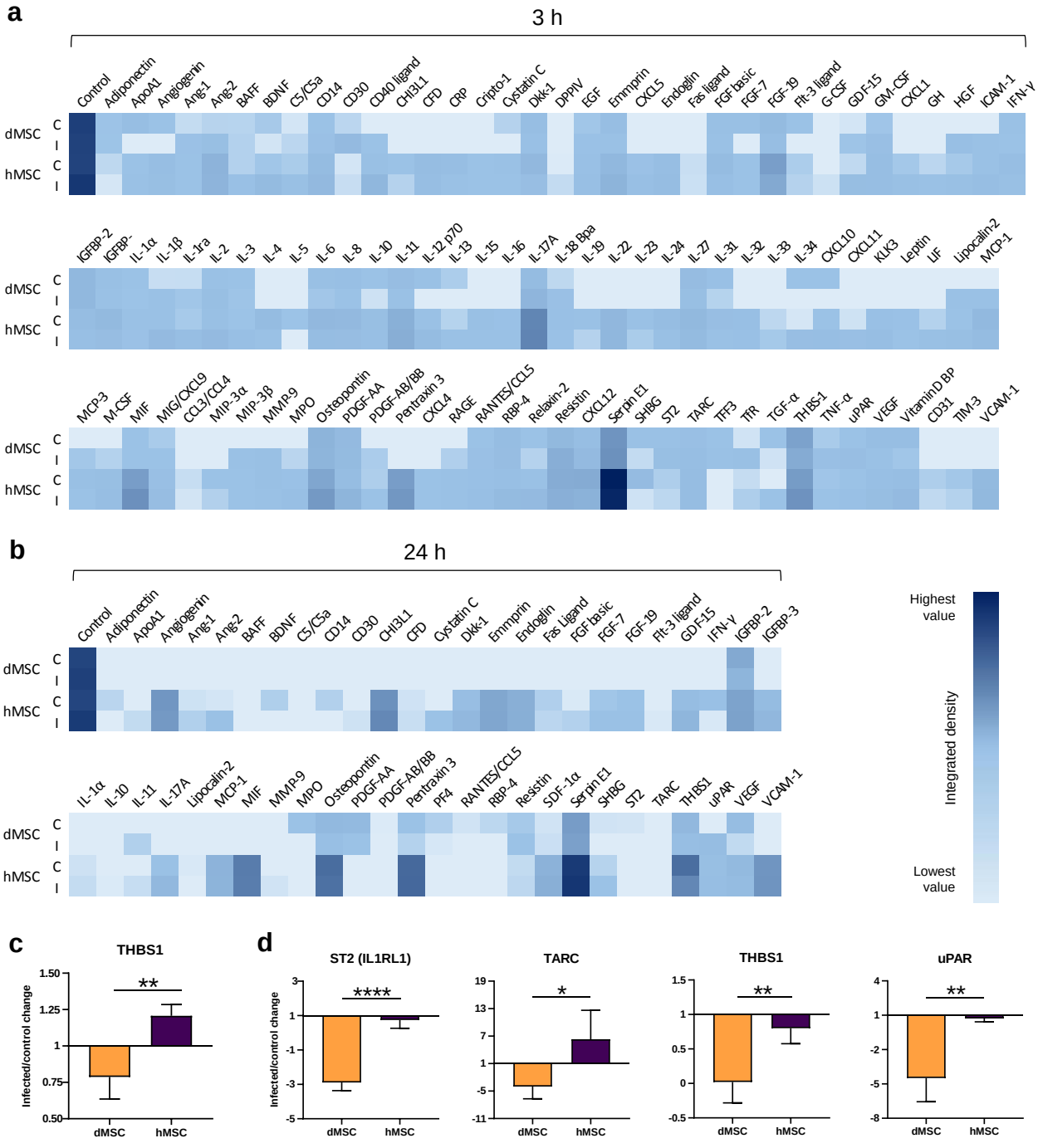
a
3 h
Control
Adiponectin
ApoA1
Angiogenin
Ang-1
Ang-2
BAFF
BDNF
C5/C5a
CD14
CD30
CD40 ligand
CHI3L1
CFD
CRP
Cripto-1
Cystatin C
Dkk-1
DPPIV
EGF
Emmprin
CXCL5
Endoglin
Fas ligand
FGF basic
FGF-7
FGF-19
Flt-3 ligand
G-CSF
GDF-15
GM-CSF
CXCL1
GH
HGF
ICAM-1
IFN-γ
IGFBP-2
IGFBP-
IL-1α
IL-1β
IL-1ra
IL-2
IL-3
IL-4
IL-5
IL-6
IL-8
IL-10
IL-11
IL-12 p70
IL-13
IL-15
IL-16
IL-17A
IL-18 Bpa
IL-19
IL-22
IL-23
IL-24
IL-27
IL-31
IL-32
IL-33
IL-34
CXCL10
CXCL11
KLK3
Leptin
LIF
Lipocalin-2
MCP-1
MCP-3
M-CSF
MIF
MIG/CXCL9
CCL3/CCL4
MIP-3α
MIP-3β
MMP-9
MPO
Osteopontin
PDGF-AA
PDGF-AB/BB
Pentraxin 3
CXCL4
RAGE
RANTES/CCL5
RBP-4
Relaxin-2
Resistin
CXCL12
Serpin E1
SHBG
ST2
TARC
TFF3
TfR
TGF-α
THBS-1
TNF-α
uPAR
VEGF
Vitamin D BP
CD31
TIM-3
VCAM-1
dMSC
hMSC
C
I
b
24 h
Control
Adiponectin
ApoA1
Angiogenin
Ang-1
Ang-2
BAFF
BDNF
C5/C5a
CD14
CD30
CHI3L1
CFD
Cystatin C
Dkk-1
Emmprin
Endoglin
Fas Ligand
FGF basic
FGF-7
FGF-19
Flt-3 ligand
GDF-15
IFN-γ
IGFBP-2
IGFBP-3
IL-1α
IL-10
IL-11
IL-17A
Lipocalin-2
MCP-1
MIF
MMP-9
MPO
Osteopontin
PDGF-AA
PDGF-AB/BB
Pentraxin 3
PF4
RANTES/CCL5
RBP-4
Resistin
SDF-1α
Serpin E1
SHBG
ST2
TARC
THBS1
uPAR
VEGF
VCAM-1
dMSC
hMSC
C
I
Highest value
Integrated density
Lowest value
c
THBS1
Infected/control change
1.50
1.25
1
0.75
0.50
**
dMSC
hMSC
d
ST2 (IL1RL1)
Infected/control change
3
1
-1
-3
-5
****
dMSC
hMSC
TARC
19
13
7
1
-5
-11
*
dMSC
hMSC
THBS1
1.5
1
0.5
0
-0.5
**
dMSC
hMSC
uPAR
4
1
-2
-5
-8
**
dMSC
hMSC

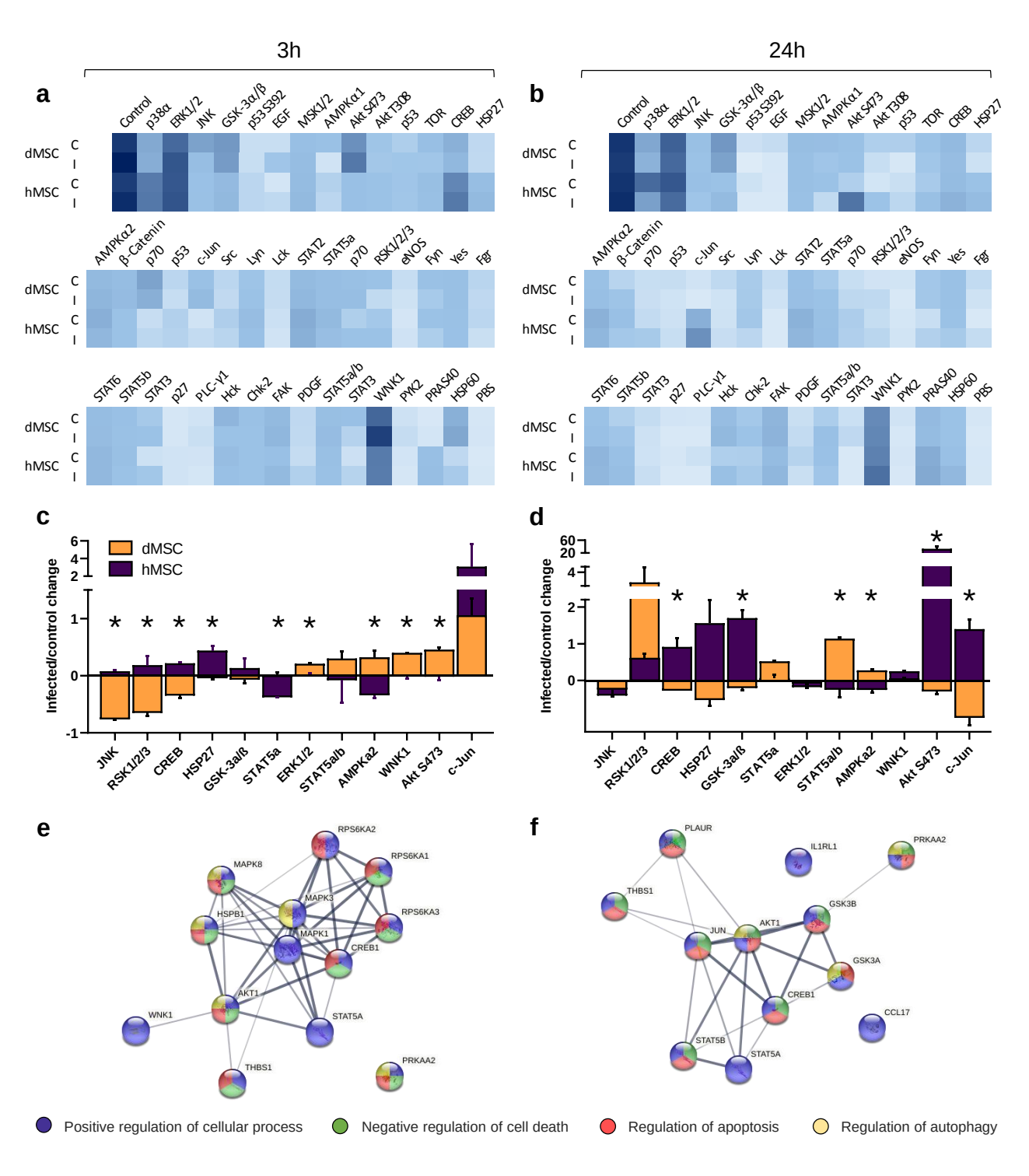
3h
24h
a
b
Control
p38α
ERK1/2
JNK
GSK-3α/β
p53S392
EGF
MSK1/2
AMPKα1
Akt S473
Akt T308
p53
TOR
CREB
HSP27
AMPKα2
β-Catenin
p70
p53
c-Jun
Src
Lyn
Lck
STAT2
STAT5a
p70
RSK1/2/3
eNOS
Fyn
Yes
Fgr
STAT6
STAT5b
STAT3
p27
PLC-γ1
Hck
Chk-2
FAK
PDGF
STAT5a/b
STAT3
WNK1
PK2
PRAS40
HSP60
PBS
dMSC
hMSC
c
d
dMSC
hMSC
Infected/control change
JNK
RSK1/2/3
CREB
HSP27
GSK-3a/ß
STAT5a
ERK1/2
STAT5a/b
AMPKa2
WNK1
Akt S473
c-Jun
e
f
RPS6KA2
RPS6KA1
MAPK8
MAPK3
HSPB1
RPS6KA3
MAPK1
CREB1
AKT1
WNK1
STAT5A
THBS1
PRKAA2
PLAUR
IL1RL1
PRKAA2
THBS1
GSK3B
AKT1
JUN
GSK3A
CREB1
CCL17
STAT5B
STAT5A
Positive regulation of cellular process
Negative regulation of cell death
Regulation of apoptosis
Regulation of autophagy

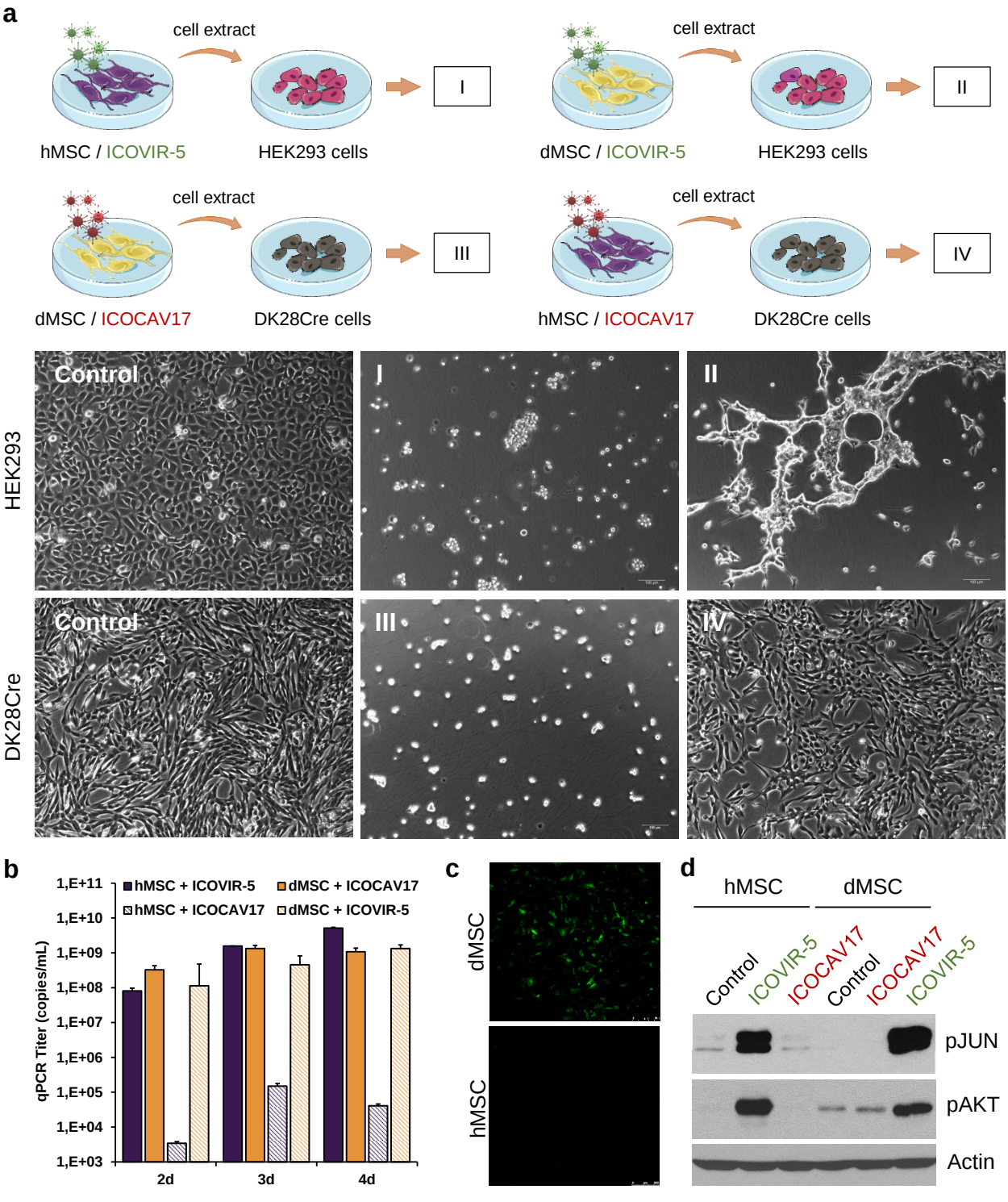
a
cell extract
hMSC / ICOVIR-5
HEK293 cells
I
cell extract
dMSC / ICOVIR-5
HEK293 cells
II
cell extract
dMSC / ICOCAV17
DK28Cre cells
III
cell extract
hMSC / ICOCAV17
DK28Cre cells
IV
HEK293
DK28Cre
Control
I
II
Control
III
IV
b
hMSC + ICOVIR-5
dMSC + ICOCAV17
hMSC + ICOCAV17
dMSC + ICOVIR-5
qPCR Titer (copies/mL)
1,E+11
1,E+10
1,E+09
1,E+08
1,E+07
1,E+06
1,E+05
1,E+04
1,E+03
2d
3d
4d
c
dMSC
hMSC
d
hMSC
dMSC
Control
ICOVIR-5
ICOCAV17
Control
ICOCAV17
ICOVIR-5
pJUN
pAKT
Actin